IEEE Access
Multidisciplinary | Rapid Review | Open Access Journal

Received October 14, 2018, accepted October 24, date of publication November 9, 2018, date of current version December 3, 2018.

Digital Object Identifier 10.1109/ACCESS.2018.2879377

Numerical Modeling and De-Embedding of Non-Planar Periodic Guided-Wave Structures via Short-Open Calibration in 3-D FEM Algorithm

YIN LI[1], SHENG SUN[2], (SENIOR MEMBER, IEEE), AND LEI ZHU[1], (FELLOW, IEEE)

[1]Department of Electrical and Computer Engineering, University of Macau, Macau 999078, China
[2]School of Electronic Science and Engineering, University of Electronic Science and Technology of China, Chengdu 61173, China

Corresponding author: Lei Zhu (leizhu@umac.mo)

This work was supported in part by the National Natural Science Foundation of China under Grant 61571468, Grant 61622106, and Grant 61721001, in part by the Macao Science and Technology Development Fund under Grant FDCT-091/2016/A2, and in part by the University of Macau under Grant CPG2017-00028-FST, Grant MYRG2018-00073-FST, and Grant MYRG2017-00007-FST.

ABSTRACT In this paper, a numerical short-open calibration (SOC) technique is presented to numerically model and de-embed a variety of non-planar periodic guided-wave structures based on the 3-D full-wave finite element method (FEM). A simple current source or lumped-port model is introduced in formulation of a determinant FEM algorithm. By incorporating the SOC in the FEM solver, the intrinsic port discontinuity caused by this port model is then fully removed or calibrated out of the core non-planar periodic guided-wave structure during the calibration process. Because of the 3-D nature of FEM, the effective per-unit-length parameters of the core periodic guided-wave structure, i.e., effective propagation constant and effective characteristic impedance, are extracted successfully. Two numerical examples, including microstrip line with periodical loading of shorting pins and metal–insulator–metal composite right/left handed structure, are numerically modeled for demonstration and verification. Extracted results have validated the feasibility and accuracy of the presented FEM-SOC, thereby exhibiting its advanced capability in numerical modeling and de-embedding of non-planar structures with complicated configurations.

INDEX TERMS Periodic guided-wave structure, characteristic impedance, propagation constant, short-open calibration, finite element method.

I. INTRODUCTION

As a basic configuration, periodic structures exhibit the guided-wave propagating behaviors and desirable properties, which have been employed in various applications, such as the electromagnetic bandgap (EBG) [1], artificial structures [2], [3], and leaky-wave antennas [4]–[7]. Numerical extraction or de-embedding of their effective per-unit-length parameters, including the complex characteristic impedances and propagation constant, has been becoming an important and indispensable procedure for efficient and effective design of advanced microwave circuits with periodic structures. In order to achieve the accurate results and high performance, numerical calibration method in full-wave algorithms is often demanded in obtaining the equivalent circuit models of these periodic structures with high degree of complexity.

According to the well-known Floquet theory, an infinite periodic structure can be characterized by solving an eigenvalue problem of a minimal periodic element, which is so-called unit cell [8]. On the one hand, various numerical methods, such as method of moment (MoM) [9], [10], finite difference frequency domain algorithm (FDTD) [11], and finite element method (FEM) [12] have been applied so far for modeling of these unit cells. However, solving an eigenvalue problem is usually time-consuming and has low efficiency, especially when more propagation modes are concerned. On the other hand, the commercial 3-D full-wave simulators, such as Ansys HFSS [13] and CST Microwave Studio [14], can provide the eigenmode solver with periodic boundary condition to directly derive the dispersion diagram of only a phase constant. With the help of the quality factor of the structures, the attenuation constant could be deduced with additional numerical efforts as descripted in [15]. Since the closed electric and magnetic boundary conditions are enforced, it always fails to directly extract the attenuation constant [15], [16], which is important for modeling of radiating structures or antennas.

As an alternative approach, the unit cell can be considered as a two-port network, where the incident and reflected waves are defined at two terminal planes and S-parameters can then be obtained. However, there exists an undesired port

discontinuity in two- or three-dimensional (2D/3D) modeling algorithms, due to the approximate source model [17]–[22] and reflected wave from the core periodic structure [23], [24]. As reported in the literature, different numerical calibration methods have been proposed to calibrate out the port discontinues and construct accurate equivalent model of the core section under modeling. By solving the eigenvalue problems of the T-matrix, the thru line (TL) calibration method was developed to extract the phase constant and attenuation constant of substrate integrated waveguide (SIW) with periodic vias [25]–[27]. Alternatively, the thru-reflect-line (TRL) was studied to characterize the SIW [28], [29]. However, this method has its fundamental limitation in its de-embedding process due to the unavoidable frequency-dependent property of the line standard. Since both the TL and TRL methods can hardly extract the Bloch-wave impedance of a periodic structure. Later on, the short-open load (SOL) [30], [31] and thru-thru (TT) [32] calibration were proposed to extract the characteristic parameters of SIW, including the Bloch-wave impedance and propagation constant. Note that the detailed information at port source should be at first defined for the SOL and TT methods. By making the even-odd-mode excitations at the electric and magnetic boundaries, the Bloch-wave impedance was extracted [16]. In this context, the port discontinuity is pre-defined as an equivalent lumped series inductance, and it needs to be estimated by simulating periodic structures with different numbers of periodic cells.

In 1997, a numerical calibration technique, namely, short-open calibration (SOC), was first proposed in [18]. With the help of two ideal open and short calibration standards in the method of moments (MoM), the de-embedding procedure can be implemented by defining the core circuit network, and two respective error boxes at two ports. Each port discontinuity and its respective feeding line are considered as an entire error box, while the effective per-unit-length parameters of the periodic structures can be accurately extracted based on the simple transmission network theory. Recently, to explore the 3D capability of the numerical de-embedding procedure, the SOC technique was implemented in the full-wave FEM algorithm [33]. By defining the reference plane along each feeding line as the perfect electric and magnetic conductors, i.e., PEC and PMC, the FEM-SOC was successfully developed without needing to take separate consideration into parasitic port errors.

In this paper, this FEM-SOC technique is further applied for numerical modeling and de-embedding of a variety of 3D periodic guided-wave structures with metallic vias. The major contribution of this work is to show the extendible capability of FEM-SOC for modeling of 3D complicated structures, which becomes important and useful for the emerging multi-layer configurations in modern microwave circuits. Especially for the metamaterial-concepted periodic structures, the extraction of effective propagation parameters including the propagation constant and characteristic impedance is absolutely necessary. As demonstration and verification, two non-planar periodic guided-wave structures,

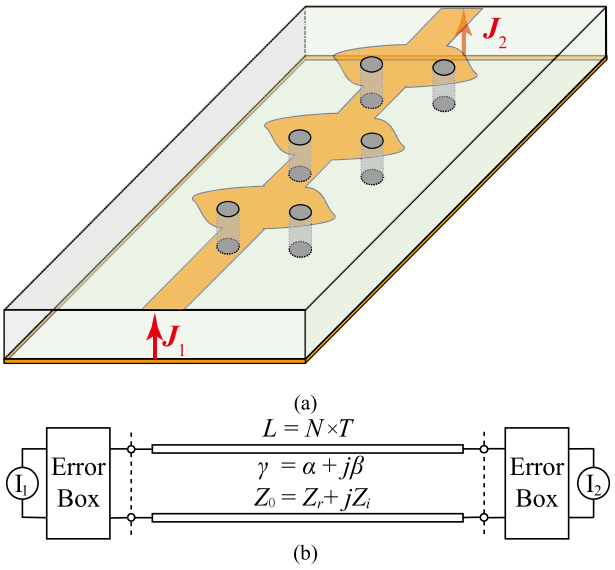

FIGURE 1. A generalized 3D non-planar periodic structure fed by an impressed current source at two ports for executing the SOC-FEM procedure. (a) Physical layout. (b) Equivalent circuit model.

i.e., microstrip line with periodical loading of shorting pins and metal-insulator-metal (MIM) composite right/left handed (CRLH) structure, are shown here. The results have evidently verified that the achieved full-wave calibration-based propagation parameters are accurate and reliable over a wide frequency range

II. FEM-SOC TECHNIQUE

Fig. 1(a) shows the physical layout for FEM–SOC modeling and de-embedding of a generalized 3D non-planar periodic guided-wave structure with metallic vias or pins, which is driven by two uniform feeding lines and impressed current sources. In the established electric-field differential equation, the unknown electric fields of the two ports can be directly solved by the FEM method as detailed in [33]. Since all the high-order modes excited by non-ideal current sources should vanish at the two reference planes, a certain distance should be properly selected between port and reference planes.

Fig. 1(b) depicts the relevant equivalent-circuit network in which the core periodic structure is equivalently perceived as the uniform dispersive and loss transmission line section [31], and the two additional sections are fed by current sourced at the two sides. Two error boxes indicate the electrical behavior of their respective current source-driven feeding lines, including all the discontinuity effects caused by the non-ideal current sources with the PMC boundary conditions at these two ports. Here, the SOC technique is used in the consistent FEM to independently characterize these two error boxes via two calibration standards, i.e., short- and open-end circuits, without predefining the equivalent network of the port discontinuity as reported in [16]. As introduced in [33] for the 2D/3D cases, these two standards are ideally realized by terminating the reference plane of each feeding line with perfect electric and magnetic walls in the FEM method,

respectively, thereby effectively constructing the ideal short- and open-end circuit standards.

In this way, the network parameters of these error boxes can be modeled in terms of the FEM-calculated equivalent voltages at the port according to the impressed current [33].

$$[X_i] = \begin{bmatrix} \dfrac{\bar{V}'_{io}\bar{V}_{is}}{\bar{V}_{io}-\bar{V}_{is}} & -\dfrac{\bar{V}'_{io}\bar{V}_{is}}{\bar{V}_{io}-\bar{V}_{is}} \\ -\dfrac{1}{\bar{V}'_{io}} & \dfrac{\bar{V}'_{io}}{\bar{V}'_{io}} \end{bmatrix} \tag{1}$$

By calibrating these error boxes out of the overall network at two ports, the core network of the central periodic structure can be extracted in a straightforward way via the cascaded topology in Fig.1. Subsequently, the effective complex characteristic impedance and propagation constant of such a non-planar periodic structure can be explicitly calculated in terms of the obtained ABCD matrix(with four elements a_p, b_p, c_p, d_p), such that

$$\cosh(\gamma L) = \frac{a_p + d_p}{2} \tag{2}$$

$$Z_0 = \sqrt{\frac{b_p}{c_p}} \tag{3}$$

where $L = N \times T$, T denotes the length of the unit cell, N is the number of unit cells of the periodic structure.

III. MODELING OF PERIODIC PIN-LOADED MICROSTRIP LINE

The pin-loaded microstrip line is a good candidate for design of the EH_0-mode microstrip leaky-wave antennas (MLWAs) [6], [7]. Compared with the higher-order EH_1/EH_2 modes, EH_0-mode MLWA owns the advantages of narrow line width, low cutoff frequency, and simple matching network.

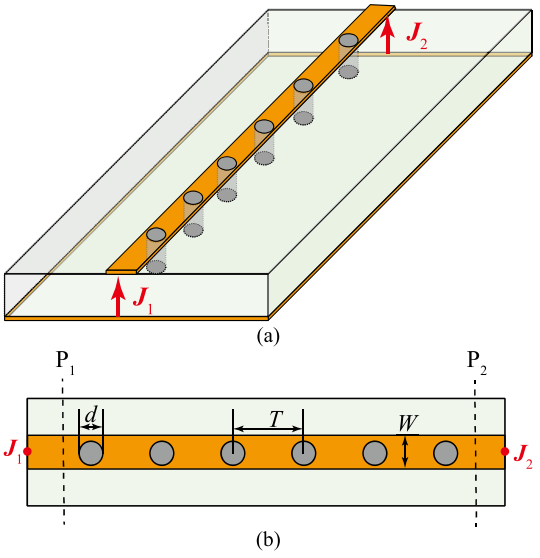

FIGURE 2. Layout of the microstrip line with periodical loading of shorting pins. (a) 3D view. (b) Top view.

Fig. 2(a) and (b) show the periodic pin-loaded microstrip line structure with N unit-cell of periodicity T. Herein, d denotes the diameter of each pin, W and L denote the width and length of the strip trace with periodical shorting pin, respectively. In this work, the dielectric substrate with relative permittivity of $\varepsilon_r = 2.5$ and height of $h = 3$ mm is used. In numerical modeling, the core circuit of microstrip line with periodical shorting pins is fed by the current source with the PMC boundary condition. For the purpose of simplification, the feeding line readily selects the same width as the periodic structure. Then, the entire network can be decomposed as two feed line sections with impressed current sources and the core periodic structure. The port discontinuity of the non-ideal current source with the PMC and the feed line are both included in the error boxes, which can be effectively evaluated and removed by employing the FEM-SOC. By using (2) and (3), the concerned effective per-unit-length transmission

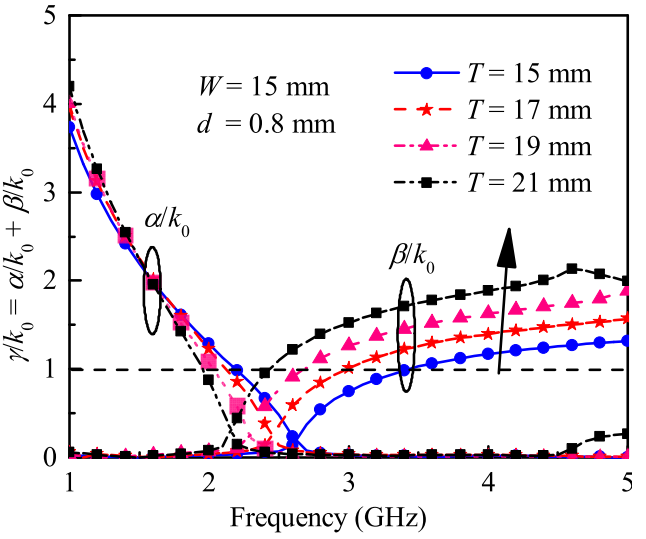

FIGURE 3. The propagation constants of pin-loaded mircrostrip line with periodicity of $d = 0.8$ mm, strip widths $W = 15$ mm and varied periodicity of T.

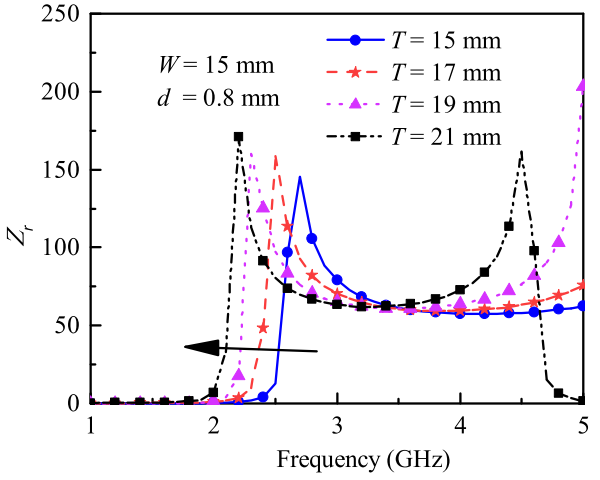

FIGURE 4. Real part of the complex characteristic impedance of the pin-loaded mircrostrip line with varied periodicity of T.

parameters of the core periodic structure can be accurately and effectively de-embedded or extracted.

Fig.3 depicts the normalized propagation constants of this non-planar periodic line with the fixed width of $W = 15$ mm and the pin's diameter of $d = 0.8$ mm. The cutoff frequency, when $\beta = \alpha$, increases as T raises from 15 to 21 mm with the interval of 2 mm. It exhibits a bandstop behavior below the cutoff frequency, where α fades away and turns to zero. Above the cutoff frequency, the pin-loaded microstrip line exhibits the fast-wave behavior, when its phase constant normalized by the free-space wavenumber is less than 1 ($\beta/k_0 < 1$), so the leaky-wave mode is excited. Meanwhile, the real part of characteristic impedance keeps near zero in the bandstop region, and it increases quickly and then decreases in the fast-wave region, as shown in Fig. 4. Afterwards, it tends to decrease and become a relative stable value in the slow-wave region above the cutoff frequency.

Fig. 5 shows the propagation constants of the pin-loaded mircrostrip line versus frequency as the diameter of shorting pins decreases from 2.0 to 0.8 mm, under the periodicity of $T = 15.0$ mm and the strip width of $W = 15$ mm. Again, the cutoff frequency is shifted downward as d is reduced. In the fast-wave propagating region, β/k_0 increases as the diameter of the pin increases, while α decreases and gradually becomes zero at the cutoff frequency as the

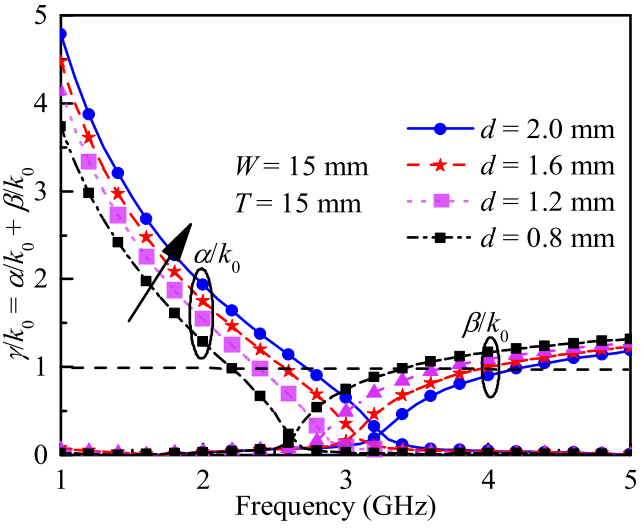

FIGURE 5. The propagation constants of pin-loaded microstrip line under periodicity of T = 15.0 mm, strip widths of W = 15 mm and varied radii of shorting pins.

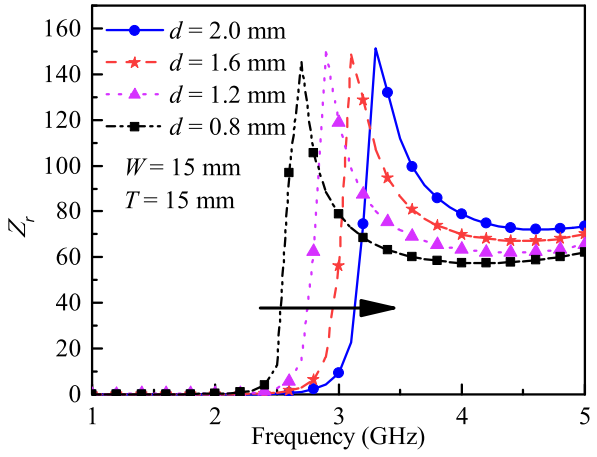

FIGURE 6. Real part of the characteristic impedance of the pin-loaded mircrostrip line under different radii of shorting pins.

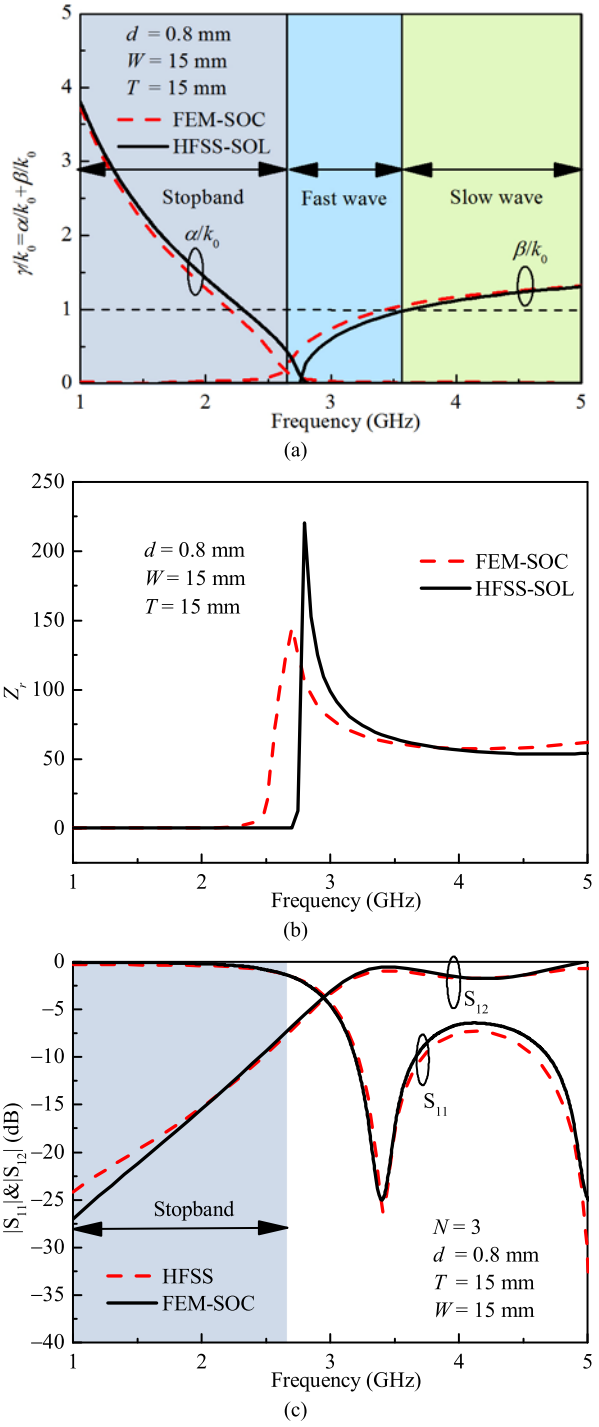

FIGURE 7. Comparison between the results of the pin-loaded mircrostrip line obtained by the FEM-SOC and HFSS-SOL/HFSS. (a) Extracted complex propagation constants. (b) Extracted real part of the characteristic impedance. (c) Calculated two-port S-parameters |S11| and |S21|.

frequency increases. As shown in Fig. 6, the real part of the characteristic impedance exhibits the similar behavior to those of T to be varied. As the diameter of shorting pins increases, the real part of the characteristic impedance beyond the fast-wave region is shifted up, and becomes relatively stable at higher frequencies. According to these pin-determined operation regions and values of the real part of characteristic impedance, the desired matching mechanism for this EH_0-mode MLWA could be properly known and realized.

Next, in order to validate the accuracy of the above-extracted parameters, the comparison between the results from the FEM-SOC and HFSS-SOL is given. The pin-loaded microstrip line under periodicity of $T = 15$ mm, strip widths of $W = 15$ mm, and pin's diameter of d $= 0.8$ mm is considered here. As shown in Fig. 7(a), the propagation constants are well matched with each other. The discrepancy in cutoff frequency between them is less than 6%, as could be seen in Fig. 7(b). This discrepancy could be attributed to the errors in numerical discretization of 3D structure in FEM, which may become undetectable for deriving the scattering parameters, as shown in Fig. 7(c).

IV. MODELING OF MIM-BASED CRLH STRUCTURE

The MIM-based CRLH structure was proposed in [34]–[36] for design of an alternative class of leaky-wave antennas. It has the unique left-handed (LH) and right-handed (RH) frequency regions, where the phase shift of per unit cell becomes negative and positive, respectively. Fig. 8(a) illustrates the perspective 3D view of the MIM CRLH periodic structure, while Fig. 8 (b) and (c) show the top view and side view of the MIM-based CRLH unit cell, respectively. It consists of three substrate layers with three metallization layers, and metallic pins or vias. The dimensions of the unit cell are denoted as $g = 0.51$ mm, $W_d = 1.1$ mm, $W_T = 1.7$ mm, $l_s = 2.99$ mm, and pin's diameter of 0.6 mm. Fig 9 depicts the frequency responses of phase constants and attenuation constants under different periodicities of $T = 3.6$, 4.2, 4.8, and 5.4 mm, respectively. For verification, the comparison in numerical modeling between the results from FEM-SOC and HFSS-SOL is provided in Fig. 9, where the periodic unit has the size of $d = 0.2$ mm and $T = 15$ mm.

As depicted in Fig. 9(a), the phase shift of per unit cell, βT, is increased from negative value in the LH region to positive value in the RH region. There is a transition in a stopband region from 7.8 to 9.5 GHz with a quasi-zero phase shift $\beta \approx 0$. In this region, the attenuation constant increases and then decreases, and this stopband often disturbs the continuous frequency scanning in application of leaky-wave antennas. The real part of characteristic impedance is plotted in Fig. 9(b). A rapid fluctuation is observed at about 9.6 GHz above this stopband, but it gradually keeps stable from 10 to 14 GHz. Next, a three-unit periodic structure without matching network is implemented and its frequency response is then calculation for verification. As shown in Fig. 9(c), the simulated S-parameters from the FEM-SOC extracted parameters and direct simulation based on the HFSS solver

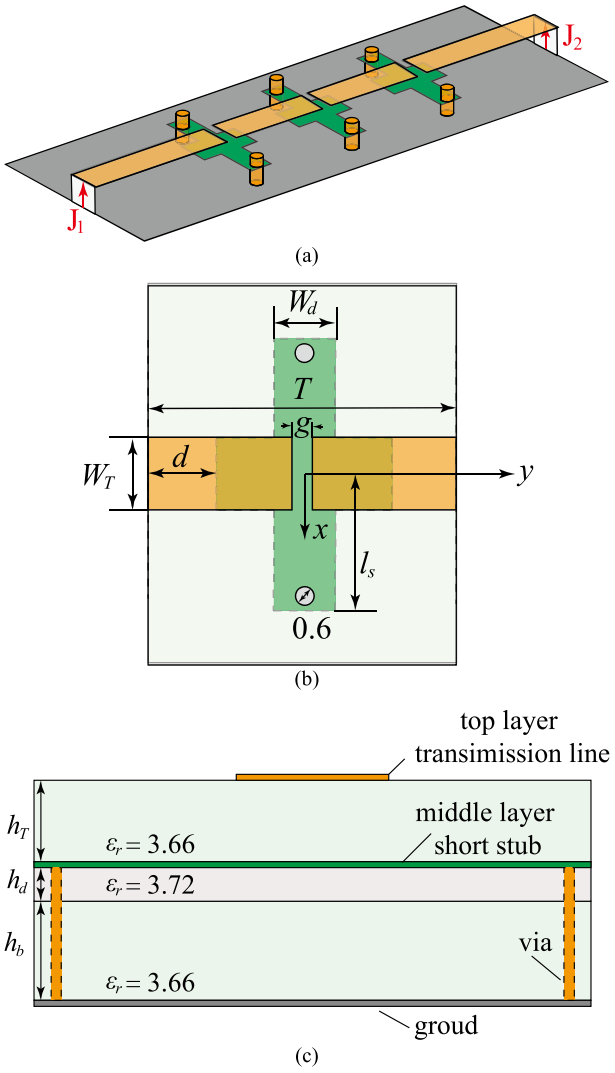

FIGURE 8. Layout of the periodic MIM-based CRLH structure. (a) Perspective view. (b) Top view of unit cell. (c) Left view of unit cell.

are in good agreement with each other, thus validating the accuracy of the proposed FEM-SOC in modeling and de-embedding of this 3D periodic structure.

Under varied periodicities of T, the extracted phase shifts per unit are intrinsically varied. As can be seen in Fig. 10(a) and (b), the transition point with $\beta = 0$ is gradually reduced as the T is enlarged, while the attenuation constant becomes more obvious as T increases from 3.6 to 5.4 mm, so this stopband increases as the T decreases. The so-called balanced condition is satisfied at $T = 3.6$ mm, where the stopband is completely eliminated. Fig. 11 shows the real part of characteristic impedances of the MIM-based CRLH periodic structure under $T = 3.6$, 4.2, 4.8, and 5.4 mm, respectively. The fluctuation of the real part of characteristic impedances around the transition point is effectively reduced as T decreases. The desired balanced condition at $T = 3.6$ mm largely increases the LH values and oppositely reduces the RH values, thus making the real part of characteristic impedances slight varied in a wide region.

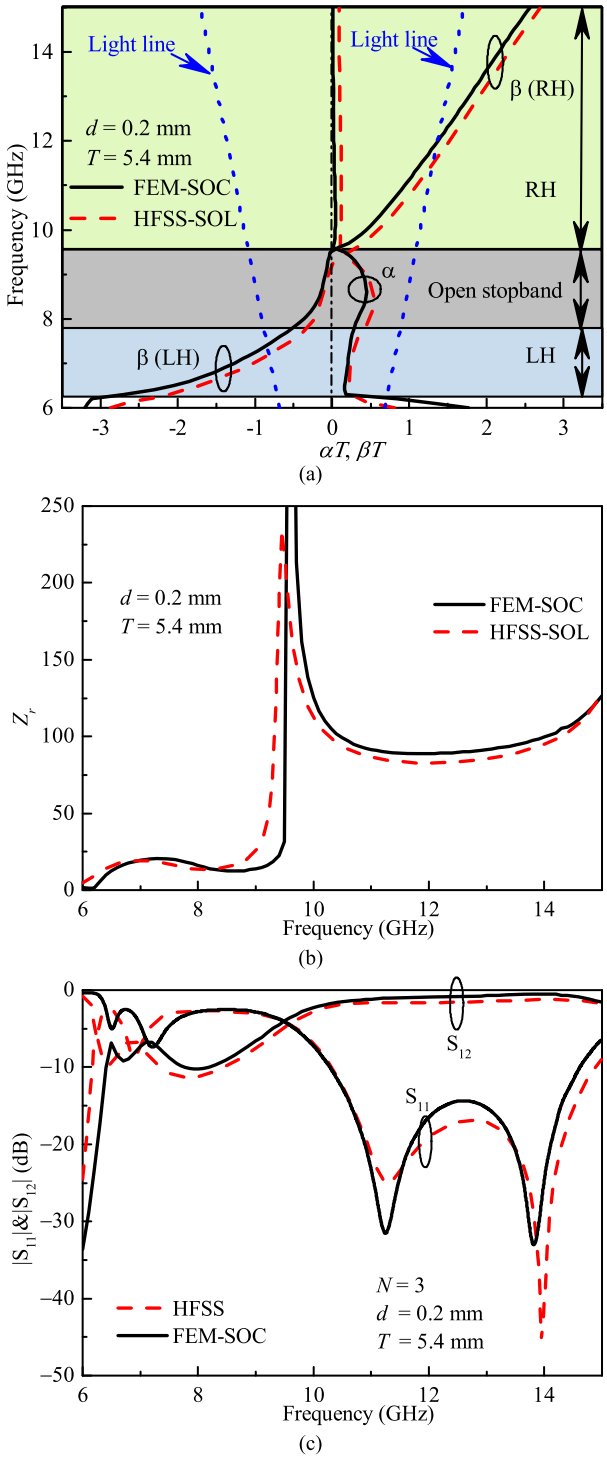

FIGURE 9. Comparison between the results of the MIM CRLH structure in Fig. 8, calculated from the FEM-SOC and HFSS-SOL/HFSS. (a) Dispersion diagram. (b) Extracted real part of the characteristic impedance. (c) Calculated two-port S-parameters |S11| and |S21|.

Next, the extracted characteristic parameters can be used to design the matching network for the MIM-based CRLH structure with finite cell units. The circuit model of the N-cell MIM-based CRLH structure in connection with two matching networks at two sides is displayed in Fig. 12. As can be seen in Fig. 13(a), at $T = 5.4$ mm, effective characteristic

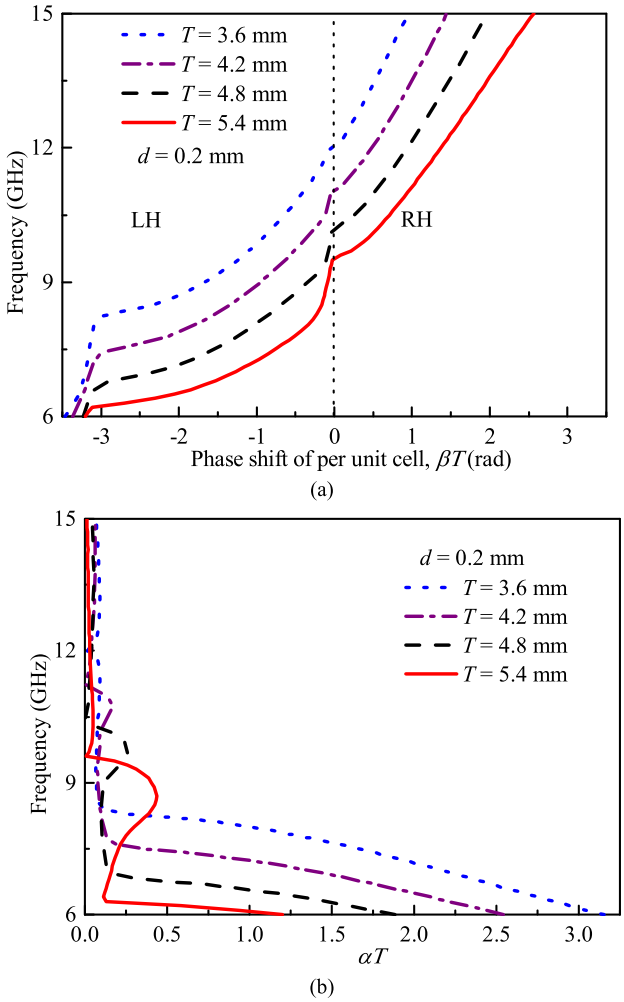

FIGURE 10. Dispersion diagram of the MIM-based CRLH structure under different periodicities of T = 3.6, 4.2, 4.8, and 5.4 mm. (a) Phase shift of per unit cell. (b) Attenuation constants.

impedances in LH and RH regions can be reasonably matched to 50 Ω by using these matching networks. Generally speaking, it is difficult to simultaneously achieve the impedance

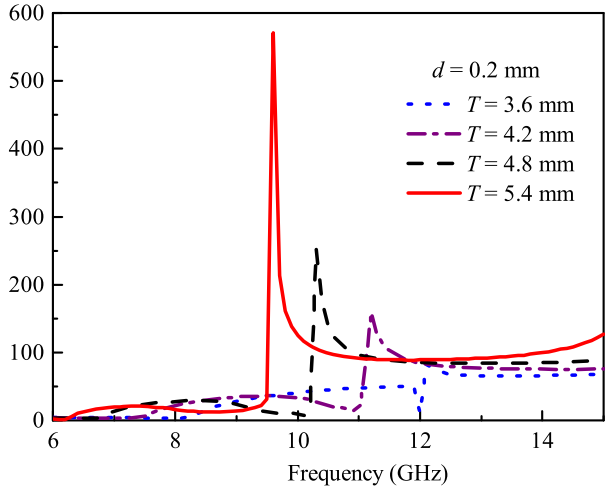

FIGURE 11. Real part of characteristic impedance of the MIM-based CRLH structure under different periodicities of T = 3.6, 4.2, 4.8, and 5.4 mm.

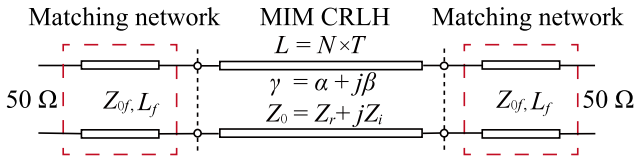

FIGURE 12. Equivalent circuit model of the MIM-based CRLH structures with two impedance matching networks at two sides.

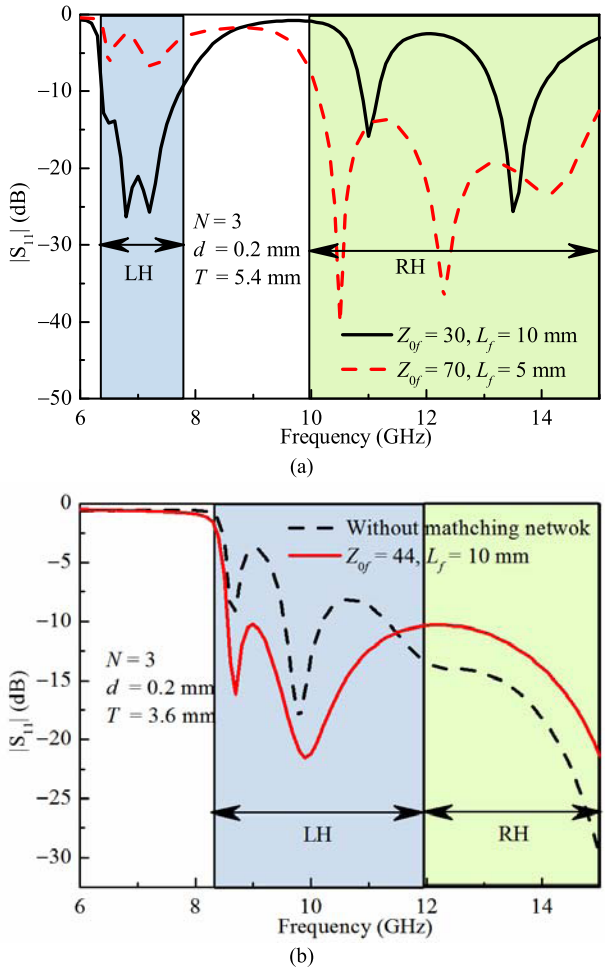

FIGURE 13. S-parameters of the MIM-based CRLH structures with different matching networks. (a) T = 5.4mm. (b) T = 3.6 mm.

match in both of the two frequency regions to the feeding lines with 50 Ω, because the characteristic impedance of a periodic guided-wave structure is highly frequency-dependent as shown in Fig. 11. However, when a balanced condition of $T = 3.6$ mm is set, good impedance matching can be achieved in both the LH and RH regions. Intrinsically, this feature is primarily due to the almost same characteristic impedances in the LH and RH regions of this MIM as illustrated in Fig. 11.

V. CONCLUSION

In this paper, numerical de-embedding and modeling of 3D non-planar periodic guided-wave structures using the FEM-SOC technique have been presented. By removing the port discontinuities and feeding network parasitic effects, effective propagation parameters of the core non-planar periodic structures with finite unit cells have been accurately determined. Through the two non-planar periodic examples, the FEM-SOC has been demonstrated to have its attractive capacity in accurate, efficient and correct modeling and de-embedding of various kinds of 3D non-planar periodic guided-wave structures. Without needing to know the predefined port discontinuity and feeding-line parasitic effect, the core network parameters of these periodic structures could be effectively de-embedded and extracted, thus it provides physical insight into their working principle and provides an effective design guideline for these 3D non-planar periodic guided-wave structures. At last, the two MIM-based CRLH structures have been modeled and designed by using the extracted per-unit-length transmission parameters from the FEM-SOC. The respective results have evidently demonstrated that the effective per-unit-length parameters can be extracted from the FEM-SOC to allow one to efficient and effective design of high-performance microwave circuits using these 3D non-planar periodic guided-wave structures.

REFERENCES

[1] F.-R. Yang, K.-P. Ma, Y. Qian, and T. Itoh, "A uniplanar compact photonic-bandgap (UC-PBG) structure and its applications for microwave circuit," *IEEE Trans. Microw. Theory Techn.*, vol. 4, no. 8, pp. 1509–1514, Aug. 1999.

[2] C. Caloz and T. Itoh, "Novel microwave devices and structures based on the transmission line approach of meta-materials," in *IEEE MTT-S Int. Microw. Symp. Dig.*, vol. 1, Jun. 2003, pp. 195–198.

[3] C. Caloz and T. Itoh, *Electromagnetic Metamaterials: Transmission Line Theory and Microwave Application*. New York, NY, USA: Wiley 2004.

[4] J. Liu, Y. Li, and Y. Long, "Design of periodic shorting-vias for suppressing the fundamental mode in microstrip leaky-wave antennas," *IEEE Trans. Antennas Propag.*, vol. 63, no. 10, pp. 4297–4304, Oct. 2015.

[5] P. Baccarelli, S. Paulotto, and D. R. Jackson, "A π-matching network to eliminate the open-stopband in 1-D periodic leaky-wave antennas," in *Proc. IEEE Int. Antennas Propag. Symp.*, Jul. 2012, pp. 1–3.

[6] D. Xie, L. Zhu, and X. Zhang, "An EH_0-mode microstrip leaky-wave antenna with periodical loading of shorting pins," *IEEE Trans. Antennas Propag.*, vol. 65, no. 7, pp. 3419–3426, Jul. 2017.

[7] J. Liu, Y. Li, and Y. Long, "Fundamental even leaky mode in microstrip line loaded with shorting vias," *IET Microw. Antennas Propag.*, vol. 1, no. 11, pp. 129–135, Jan. 2017.

[8] R. E. Collin, *Foundation of Microwave Engineering*, 1st ed. New York, NY, USA: McGraw-Hill, 1966.

[9] S. Marini, Á. Coves, V. E. Boria, and B. Gimeno, "Full-wave modal analysis of slow-wave periodic structures loaded with elliptical waveguides," *IEEE Trans. Electron. Devices*, vol. 57, no. 2, pp. 516–524, Feb. 2010.

[10] G. I. Zaginaylov, A. Hirata, T. Ueda, and T. Shiozawa, "Full-wave modal analysis of the rectangular waveguide grating," *IEEE Trans. Plasma Sci.*, vol. 28, no. 3, pp. 614–620, Jun. 2000.

[11] F. Xu, K. Wu, and W. Hong, "Equivalent resonant cavity model of arbitrary periodic guided-wave structures and its application to finite-difference frequency-domain algorithm," *IEEE Trans. Microw. Theory Techn.*, vol. 55, no. 4, pp. 697–702, Apr. 2007.

[12] S. Giani, "Convergence of adaptive finite element methods for elliptic eigenvalue problems with applications to photonic," Ph.D. dissertation, Univ. Bath, Bath, U.K., 2008.

[13] *CST Computer Simulation Technology*. [Online]. Available: http://www.cst.com/

[14] ANSYS. [Online]. Available: https://www.ansys.com

[15] A. J. Martinez-Ros and F. Mesa, "A study on the dispersion relation of periodic structures using commercial simulators," in *Proc. Comput. Electromagn. Int. Workshop*, Jun. 2017, pp. 15–16.

[16] M. A. Eberspächer and T. F. Eibert, "Dispersion analysis of complex periodic structures by full-wave solution of even-odd-mode excitation problems for single unit cells," *IEEE Trans. Antennas Propag.*, vol. 61, no. 12, pp. 6075–6083, Dec. 2013.
[17] J. C. Rautio, "A de-embedding algorithm for electromagnetics," *Int. J. RF Microw. Comput.-Aided Eng.*, vol. 1, no. 3, pp. 282–287, Jul. 1991.
[18] J. C. Rautio, "Deembedding the effect of a local ground plane in electromagnetic analysis," *IEEE Trans. Microw. Theory Techn.*, vol. 53, no. 2, pp. 770–776, Feb. 2005.
[19] J. C. Rautio and V. I. Okhmatovski, "Unification of double-delay and SoC electromagnetic deembedding," *IEEE Trans. Microw. Theory Techn.*, vol. 53, no. 9, pp. 2892–2898, Sep. 2005.
[20] L. Zhu and K. Wu, "Line-to-ring coupling circuit model and its parametric effects for optimized design of microstrip ring circuits and antennas," in *IEEE MTT-S Int. Microw. Symp. Dig.*, Jun. 1997, pp. 289–292.
[21] L. Zhu and K. Wu, "Unified equivalent-circuit model of planar discontinuities suitable for field theory-based CAD and optimization of M(H)MIC's," *IEEE Trans. Microw. Theory Techn.*, vol. 47, no. 9, pp. 1589–1602, Sep. 1999.
[22] L. Zhu and K. Wu, "Network equivalence of port discontinuity related to source plane in a deterministic 3-D method of moments," *IEEE Microw. Guided Wave Lett.*, vol. 8, no. 3, pp. 130–132, Mar. 1998.
[23] F. Xu, K. Wu, and W. Hong, "Domain decomposition FDTD algorithm combined with numerical TL calibration technique and its application in parameter extraction of substrate integrated circuits," *IEEE Trans. Microw. Theory Techn.*, vol. 54, no. 1, pp. 329–338, Jan. 2006.
[24] F. Xu and K. Wu, "Guided-wave and leakage characteristics of substrate integrated waveguide," *IEEE Trans. Microw. Theory Techn.*, vol. 53, no. 1, pp. 66–73, Jan. 2005.
[25] L. Han, K. Wu, X.-P. Chen, and F. He, "Accurate analysis of finite periodic substrate integrated waveguide structures and its applications," in *IEEE MTT-S Int. Microw. Symp. Dig.*, May 2010, pp. 864–867.
[26] K. W. Eccleston, "A new interpretation of through-line deembedding," *IEEE Trans. Microw. Theory Techn.*, vol. 64, no. 11, pp. 3887–3893, Nov. 2016.
[27] K. W. Eccleston, "Verification of extended through-line deembedding," in *Proc. Asia Pacific Microw. Conf.*, Nov. 2017, pp. 1276–1279.
[28] E. D. Caballero, A. Belenguer, H. Esteban, and V. E. Boria, "Thru-reflect-line calibration for substrate integrated waveguide devices with tapered microstrip transitions," *Electron. Lett.*, vol. 49, no. 2, pp. 132–133, Jan. 2013.
[29] X.-P. Chen and K. Wu, "Accurate and efficient design approach of substrate integrated waveguide filter using numerical TRL calibration technique," in *IEEE MTT-S Int. Microw. Symp. Dig.*, Jun. 2008, pp. 1231–1234.
[30] Q.-S. Wu and L. Zhu, "Numerical de-embedding of effective wave impedances of substrate integrated waveguide with varied via-to-via spacings," *IEEE Microw. Wireless Compon. Lett.*, vol. 26, no. 1, pp. 1–3, Jan. 2016.
[31] L. Zhu, Q.-S. Wu, and S.-W. Wong, "Numerical SOC/SOL calibration technique for de-embedding of periodic guided-wave structures," in *Proc. IEEE Int. Conf. Comput. Electromagn. (ICCEM)*, Feb. 2016, pp. 325–327.
[32] F. Fesharaki, T. Djerafi, M. Chaker, and K. Wu, "S-parameter deembedding algorithm and its application to substrate integrated waveguide lumped circuit model extraction," *IEEE Trans. Microw. Theory Techn.*, vol. 65, no. 4, pp. 1179–1190, Apr. 2017.
[33] Y. Li and L. Zhu, "A short–open calibration method for accurate de-embedding of 3-D nonplanar microstrip line structures in finite-element method," *IEEE Trans. Microw. Theory Techn.*, vol. 66, no. 3, pp. 1172–1180, Mar. 2018.
[34] M. Kang, C. Caloz, and T. Itoh, "Miniaturized MIM CRLH transmission line structure and application to backfire-to-endfire leaky-wave antenna," in *Proc. IEEE Antennas Propag. Soc. Int. Symp.*, vol. 1, Jun. 2004, pp. 827–830.
[35] S. Otto, Z. Chen, A. Al-Bassam, A. Rennings, K. Solbach, and C. Caloz, "Circular polarization of periodic leaky-wave antennas with axial asymmetry: Theoretical proof and experimental demonstration," *IEEE Trans. Antennas Propag.*, vol. 62, no. 4, pp. 1817–1829, Apr. 2014.
[36] S. Otto, A. Al-Bassam, A. Rennings, K. Solbach, and C. Caloz, "Transversal asymmetry in periodic leaky-wave antennas for Bloch impedance and radiation efficiency equalization through broadside," *IEEE Trans. Antennas Propag.*, vol. 62, no. 10, pp. 5037–5054, Oct. 2014.

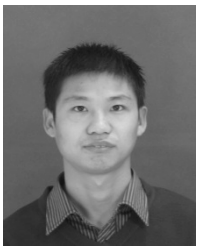

YIN LI received the B.S. degree in applied physics from the China University of Petroleum, Dongying, China, in 2009, and the M.Eng. degree in electromagnetic field and microwave technology from the University of Electronic Science and Technology of China, Chengdu, China, in 2012. He is currently pursuing the Ph.D. degree with the University of Macau, Macau, China.

From 2013 to 2015, he was a Research Assistant with The University of Hong Kong, Hong Kong. His current research interests include numerical modeling methods of passive microwave circuits, computational electromagnetics, and microwave circuits.

SHENG SUN (S'02–M'07–SM'12) received the B.Eng. degree in information engineering from Xi'an Jiaotong University, Xi'an, China, in 2001, and the Ph.D. degree in electrical and electronic engineering from Nanyang Technological University (NTU), Singapore, in 2006.

He was a Post-Doctoral Research Fellow with the Institute of Microelectronics, Singapore, from 2005 to 2006, and NTU from 2006 to 2008. He was a Humboldt Research Fellow with the Institute of Microwave Techniques, University of Ulm, Germany, from 2008 to 2010, and a Research Assistant Professor with The University of Hong Kong from 2010 to 2015. Since 2015, he has been a Full Professor with the University of Electronic Science and Technology of China. He has coauthored one book and two book chapters, over 140 journal, and conference publications. His research interests include electromagnetic theory and computational mathematics, multi-physics, numerical modeling of planar circuits and antennas, microwave passive and active devices, as well as the microwave and millimeter-wave communication systems.

Dr. Sun is currently a member of the Editor Board of *International Journal of RFMiCAE* and the *Journal of Communications and Information Networks*. He was a co-recipient of the several best paper awards at international conferences. He received the ISAP Young Scientist Travel Grant (Japan), in 2004, and the Hildegard Maier Research Fellowship of the Alexander Von Humboldt Foundation (Germany), in 2008. He also received the Outstanding Reviewer Award from the IEEE Microwave and Wireless Components Letters in 2010. He was a recipient of the General Assembly Young Scientists Award from the International Union of Radio Science in 2014. He was an Associate Editor of the *IEICE Transactions on Electronics* from 2010 to 2014 and the Guest Associate Editor of the ACES Journal in 2017. He is also an Associate Editor of the IEEE Microwave and Wireless Components Letters.

LEI ZHU (S'91–M'93–SM'00–F'12) received the B.Eng. and M.Eng. degrees in radio engineering from the Nanjing Institute of Technology (Southeast University), Nanjing, China, in 1985 and 1988, respectively, and the Ph.D. degree in electronic engineering from the University of Electro-Communications, Tokyo, Japan, in 1993.

From 1993 to 1996, he was a Research Engineer with Matsushita-Kotobuki Electronics Industries Ltd., Tokyo. From 1996 to 2000, he was a Research Fellow with the École Polytechnique de Montréal, Montreal, QC, Canada. From 2000 to 2013, he was an Associate Professor with the School of Electrical and Electronic Engineering, Nanyang Technological University, Singapore. In 2013, he joined the Faculty of Science and Technology, University of Macau, Macau, China, as a Full Professor, where he has been a Distinguished Professor since 2016. From 2014 to 2017, he served as the Head of the Department of Electrical and Computer Engineering, University of Macau. He has authored or co-authored more than 460 papers in international journals and conference proceedings. His papers have been cited more than 5750 times with the H-index of 41 (source: ISI Web of Science). His research interests include microwave circuits, guided-wave periodic structures, planar antennas, and computational electromagnetic techniques.

Dr. Zhu served as a member of the IEEE MTT-S Fellow Evaluation Committee from 2013 to 2015 and the IEEE AP-S Fellows Committee from 2015 to 2017. He was a recipient of the 1993 First-Order Achievement Award in Science and Technology from the National Education Committee, China, the 1996 Silver Award of Excellent Invention from Matsushita-Kotobuki Electronics Industries Ltd., and the 1997 Asia–Pacific Microwave Prize Award. He served as the General Chair of the 2008 IEEE MTT-S International Microwave Workshop Series on the Art of Miniaturizing RF and Microwave Passive Components, Chengdu, China, and the Technical Program Committee Co-Chair of the 2009 Asia–Pacific Microwave Conference, Singapore. He was an Associate Editor of the IEEE MICROWAVE AND WIRELESS COMPONENTS LETTERS from 2006 to 2012 and the IEEE TRANSACTIONS ON MICROWAVE THEORY AND TECHNIQUES from 2010 to 2013.